




*I would like to dedicate this thesis to my family who has supported
and encouraged me throughout this endeavor: Thank you for your
love and support throughout my entire life and helping me to
realize who I am today*

CERTIFICATE

It is certified that the work contained in the thesis titled “**Porous Polymeric Membrane for Fuel Cell and Radionuclide Waste Management**” by “*Om Prakash*” has been carried out under my supervision and that this work has not been submitted elsewhere for a degree.

It is further certified that the student has fulfilled all the Comprehensive, Candidacy and SOTA requirements for the award of a PhD degree.

Date: **07 July 2021**
Place: IIT (BHU), Varanasi


Prof. Pralay Maiti
(Supervisor)

DECLARATION BY THE CANDIDATE

I, **Om Prakash**, certify that the work embodied in this thesis is my own bonafide work and carried out by me under the supervision of **Prof. Pralay Maiti** from **January 2016 to June 2021** at the **School of Materials Science & Technology**, Indian Institute of Technology, Banaras Hindu University, Varanasi. The matter embodied in this thesis has not been submitted for any other degree/diploma award. I declare that I have faithfully acknowledged and given credits to the research workers wherever their works have been cited in my work in this thesis. I further say that I have not willfully copied any other's work, paragraphs, text, data, results, etc., reported in journals, books, magazines, reports, dissertations, theses, etc., or available at websites and have not included them in this thesis and have not cited as my own work.

Date: 07 July 2021

Place: Varanasi



(Om Prakash)

Certificate by the Supervisor(s)

It is certified that the above statement made by the student is correct to the best of my knowledge.



(Pralay Maiti)
Supervisor

(Chandana Rath)
Coordinator

COPYRIGHT TRANSFER CERTIFICATE

Title of the Thesis: Porous Polymeric Membrane for Fuel Cell and Radionuclide Waste Management

Name of the Student: Om Prakash

Copyright Transfer

The undersigned hereby assigns to the Indian Institute of Technology (Banaras Hindu University) Varanasi all rights under copyright that may exist in and for the above thesis submitted for the “Doctor of Philosophy” award.

Date: 07 July 2021



Place: Varanasi

(Om Prakash)

Note: However, the author may reproduce or authorize others to reproduce material extracted verbatim from the thesis or derivative of the thesis for the author's personal use. The source and the Institute's copyright notice are indicated.

ACKNOWLEDGEMENT

It's my pleasure to acknowledge the help, support, encouragement, and guidance that I have received from the number of peoples in completing the thesis.

*I am incredibly grateful to my research guide, **Professor Pralay Maiti, Professor, School of Materials Science and Technology, IIT (BHU), Varanasi, for his valuable guidance, scholarly inputs, and consistent encouragement** throughout the research work. This work was possible only because of his scientific vision and unconditional support. I have spent more than five years in the School of Materials Science and Technology, IIT (BHU), Varanasi. During this period, I learned many things along with research work which I hope will be helpful in my life. I would like to thank all the respected teachers of the school, **Prof. Dhananjay Pandey, Prof. Rajiv Prakash, Dr. Chandana Rath, Dr. Akhilesh Kr. Singh, Dr. Chandan Upadhyay, Dr. Bholanath Pal, Dr. Ashish Kumar Mishra, Dr. Shrawan Mishra, Dr. Sanjay Singh and Dr. Nikhil Kumar** for their valuable suggestions and encouragement during research work.*

I am also grateful to my Research Program Evaluation Committee (RPEC) members, Professor Nira Misra from School of biomedical Engineering and Professor K. D. Mandal from the Department of Chemistry, IIT (BHU).

I am obliged and grateful to Prof. D.K Avasthi and Dr. Saif A. Khan Inter-University Accelerator Centre, New Delhi, for their support during irradiation experiments. I would like to thank Dr. Vinod K. Shahi, Central Salt and Marine Chemical Research Institute, Gujarat, to provide DMFCs and proton conductivity facilities. I would also like to thank Prof. A.K Pandey, Dr. Rahul Tripathi, and Dr. Amol M. Mhatre BARC Mumbai for their support radionuclide related experiments. Thanks to my co-workers Dr. Karun Kumar Jana and Mr. Shivam Tiwari for their constant support. I also thank

to my labmates Dr. Dinesh Kumar Patel, Dr. Sunil Kumar, Dr. Akhand Pratap Singh, Dr. Arun Kumar Mahanta, Dr. Sudipta Senapati, Dr. Arpan Biswas, Dr. Anupama Gaur, Dr. Aparna Shukla. Ms. Dipti Saxena, Mr. Sunil Kumar, My juniors, Mr. Shyam Bihari, Ms. Reshu Bhardwaj, Mr. Ravi Prakash, Mr. Pravesh Kumar Yadav, Mr. Swapan Maity, Ms. Sudepta Bauri and Ms. Swikriti Tripathi for the cooperation and pleasant company. I gratefully acknowledge Central Instrumental Facility Centre, IIT (BHU), Varanasi, for providing various instrumental facilities.

I express my sincere gratitude to all my family members who have encouraged and motivated me for higher studies and supported my decision to do a PhD. I would also like to thank one of my family members, Aditi Yadav, who is equal to a friend as well. I am also greatly indebted to my friends Mr. Ravi Prakash Ojha, Mr. Vineet Kumar Mall, Mr. Vineet Dixit, Mr. Suneet Dixit, Ms. Rahul Upadhyay and Dr. Richa Mishra. I am thankful to my school's technical and non-technical staff for their cooperation at all level. Finally, I gratefully acknowledge the UGC and Council of Scientific and Industrial Research (CSIR), India, to provide me with financial assistance. Last but not least, I express my deep sense of gratitude to Almighty God; without his divine grace and blessing, above all, this task would have been virtually impossible.

Date: 07.07.2021

Place: Varanasi



(Om Prakash)

TABLE OF CONTENTS

Chapter 1: Introduction and literature survey

1.1 Introduction:.....	1
1.2 Polymeric membrane:	2
1.3 Nanohybrid membrane (NH):	3
1.4 PVDF and its copolymers:	4
1.5 Ions exchange membrane:.....	6
1.5.1 Cationic exchange membranes (CEMs):.....	7
1.5.2 Anion Exchange membranes (AEMs):	9
1.5.3 Bipolar membranes (BPMs):	10
1.6 Various Techniques used for the Fabrications of the Ionic membrane:	11
1.6.1 Functionalized membrane preparation via radiation induced grafting:	11
1.6.2 Functionalized to prepare chemical modified membrane:	13
1.6.3 Blend /composites membrane:.....	14
1.7 Swift Heavy ions (SHI):.....	16
1.7.1 Physical changes after the SHI:	17
1.7.2 Chemical changes after the SHI:.....	18
1.7.3 Chemical etching and formations of the Latent track:	19
1.7.4 Fabrications of the conducting nanochannels:	20
1.8 Applications of the ionic membrane:	21
1.8.1 Fundamentals of Fuel cell Technology and working Principle:	21
1.8.2 Polymer Electrolytes fuel cell membrane:	24
1.8.3 Direct Methanol fuel cell (DMFCs).....	25
1.9 Nafion membrane (Commercial)	26
1.9.1 Advantages:.....	27
1.9.2 Disadvantages:	28
1.9.3 Developments:	28
1.10 Ionic membrane in field of the nuclear waste management's:.....	28
1.11 Literature survey on uniform latent track fabrication:	29
1.12 Literature survey on Ionic Membrane characteristics:.....	33
1.13 Literature survey for Polymer electrolytes membrane and fuel cell efficiency:.....	35
1.14 Literature survey on the Radionuclide managements and tracing:	36

1.15 Motivation of the works and objective of the present work:	37
---	----

Chapter 2: Materials, Experiments and Characterization

2.1 Materials	39
2.1.1 Polymers:	39
2.1.2 Organically modified Nanoclay and monomer solutions:	39
2.1.3 Regents and Solvents:	40
2.2 Experiments	41
2.2.1 Preparation of pristine membrane and Nanohybrid:	41
2.2.2 Direct Functionalization of the Pristine Polymer:	42
2.2.3 Fabrication of the Nanochannel via the Particle radiation swift Heavy ions:....	43
2.2.4 Functionalization of the nanochannel formed by Swift Heavy ions:.....	43
2.3 Characterizations Techniques	44
2.3.1 Field emission scanning electron microscopy (FE-SEM):	45
2.3.2 Atomic Force Microscopy (AFM):.....	45
2.3.3 Polarizing Optical microscope (POM):	46
2.3.4 Ultra-violet visible (UV-vis) spectroscopy:.....	46
2.3.5 Fourier-transform infrared (FTIR) spectroscopy:	46
2.3.6 Nuclear Magnetic resonance (NMR):.....	47
2.3.7 XRD for structural modifications:	47
2.3.8 Thermogravimetric analysis (TGA):.....	48
2.3.9 Differential scanning calorimetry (DSC):.....	48
2.3.10 Ion exchange capacity of the membranes using radionuclide tracer:	48
2.3.11 Water uptake (WU):.....	49
2.3.12 Mechanical Testing:.....	49
2.4 Quantification of Radionuclide Waste.....	49
2.4.1 Sorption studies:.....	49
2.4.2 Alpha spectrometry study:	50
2.4.3 Alpha track radiography:	50
2.5 Electrochemical Analysis.....	51
2.5.1 Electrochemical impedance spectroscopy (EIS):.....	51
2.5.2 Activation energy:.....	51
2.5.3 Linear Polarization Studies:	52
2.5.4 Methanol Permeability:.....	52

2.5.4 Membrane Electrode Assembly (MEA):	53
Chapter 3: Functionalization poly(vinylidene fluoride-co-hexafluoro propylene) Membrane for Fuel cell	
3.1 Introduction:.....	55
3.2 Experimental.....	57
3.2.1 Materials:	57
3.2.2 Functionalization of the membrane:	57
3.3 Results and discussion	58
3.3.1 Ionomer preparation:.....	58
3.2.2 Structure and morphological changes due to functionalization:.....	62
3.3.3 Thermal, mechanical and electrical properties:	63
3.3.4 Proton conductivity and methanol permeability of functionalized membrane:	65
3.3.5 Fuel cell efficiency using functionalized membrane:	68
3.4 Conclusion:	69
Chapter 4: Fabrication of low cost poly(vinylidene Fluoride) Nanohybrid Membrane for superior Fuel cell	
4.1 Introduction:.....	71
4.2 Experimental.....	74
4.2.1 Materials:	74
4.2.2 Functionalization of the membrane:	74
4.3 Results and discussion	76
4.3.1 Nanochannel fabrication:	76
4.3.2 Grafting of PVDF and functionalization within the nanochannel:	78
4.3.3 Structural modifications:.....	82
4.3.4 Effect of functionalization on thermal and electrical properties:.....	85
4.3.5 Proton conductivity and methanol permeability of the functionalized membrane:.....	88
4.3.6 Fuel cell efficiency in MEA stack:	91
4.4 Conclusion	93
Chapter 5: Fabrication of Conducting Nanochannels using Accelerator for Fuel cell Membrane and Removal of Radionuclide's: Role of Nanoparticles	
5.1 Introduction:.....	95
5.2 Experimental.....	97
5.2.1 Materials:	97

5.2.2 Functionalization of the membrane:	98
5.4 Results and discussion:	99
5.3.1 Nanochannel fabrication using swift heavy ions:	99
5.3.2 Functionalization of nanochannels:	102
5.3.3 Functionalization induced structural change:	106
5.3.4 Electrochemical analysis and functionalized material as corrosion inhibitor: ..	109
5.3.5 Separation of radionuclide from waste and fundamentals:	113
5.3.6 Fuel cell performance using functionalized membranes:	116
5.4 Conclusions.....	120
Chapter 6: Lithium Irradiated poly (vinylidene fluoride) Nanohybrid Membrane for radionuclide Waste Management and Tracing	
6.1 Introduction:.....	123
6.2 Experimental	126
6.2.1 Materials:	126
6.2.2 Functionalization of the membrane:	126
6.3 Results and discussion:	129
6.3.1 Fabrication of nanochannels using SHI:	129
6.3.2 Functionalization and evolving of interactive system:	133
6.3.3 Structural modifications and thermal properties:.....	137
6.3.4 Membrane characteristics and electrochemical analysis:	140
6.3.5 Radionuclide uptake.....	143
6.3.6 Depth profiling of radionuclide within nanochannels:	145
6.3.7 Sensing of radionuclide using functionalized film:	149
6.4 Conclusions:.....	150
Chapter 7: Conclusions and Scope of the work	
7.1 Conclusions:.....	153
7.2 Scope for future work:	156
References.....	157
List of Publications	181

LIST OF FIGURE

Figure 1.1: Various membranes based on the pore size.....	2
Figure 1.2: Preparation of Nanohybrid membrane.....	4
Figure 1.3: Schematic representation of the (a) α -trans gauche conformation; (b) β -all trans conformation of crystalline PVDF, while the black, pink and yellow spheres represent carbon, hydrogen and fluorine atoms, respectively. The arrows signify $-CF_2$ dipole directions.....	5
Figure 1.4: Cation exchange membrane.....	9
Figure 1.5: Anion Exchange membrane.....	9
Figure 1.6: Schematic Presentation of BPM.....	10
Figure 1.7: Schematic of the chemical changes after the Swift Heavy Ions bombardments.....	19
Figure 1.8: Schematic presentation of a fuel cell set-up.....	22
Figure 1.9: Working principle and cell reaction based Schematic of the DMFCs.....	26
Figure 1.10 Chemical structure of the Nafion.....	27
Figure 1.11: Morphological studies (a) SEM mages of the HFP and its nanohybrid membrane with various fluence: (b) channel distribution analysis using the image-j software after the chemical etching; (c) AFM morphology of HFP-e and NH-e at a fluence of 5×10^{10} ion/cm ²	30
Figure 1.12: Surface latent track after the variation of the temperature keeping the ions (¹²⁹ Xe) and fluence is constant and chemical etchant used alkaline KMnO ₄ (a) 120 °C	

channel dimensions ~ 180 nm (b) 25 °C channel dimension ~ 120 nm (c) -84 °C channel dimension ~ 100 nm.....32

Figure 2.1: Structure of (a) organic modifier used in 30B; (b) styrene monomer; (c) 3-hexyl thiophene monomer.....40

Figure 2.2: Nanohybrid preparation by solution route.....41

Figure 2.3: Schematic of the direct Functionalization.....42

Figure 2.4: Schematic of the Radiation induced grafting.....44

Figure 3.1: (a) ¹H NMR spectra of HFP and sulfonated membranes with the assignment of their characteristic peaks position; (b) FTIR spectra of pure HFP and its functionalized membranes and indicate the extra peak arises after the sulphonation using vertical lines; (c) UV-visible absorption spectra of the HFP, HFP-12 and HFP-18 indicating the peak position; and (d-f) are overlay EDS mapping of the HFP, HFP-12, and HFP-18, respectively (from left to right), the red spot indicate the position of sulphur atom; (g) EDX spectra of the HFP, HFP-12 and HFP-18 are respectively.....60

Figure 3.2: (a) XRD spectra of HFP, HFP-12 and HFP-18 indicating the crystalline planes; (b) polarizing optical images of spherulitic morphology of HFP and HFP-18 membrane indicating the position γ -spherulite by arrows; (c) AFM images for surface morphology of HFP and HFP-18; (d) average height profile of HFP and HFP-18 membranes.....62

Figure 3.3: (a) Thermo-gravimetric analysis (TGA) of pristine HFP and functionalized HFP-12, and HFP-18 membranes; (b) differential scanning calorimetric (DSC) thermogrammes of HFP, HFP-12, and HFP-18 for the determination of melting point; (c) stress-strain curves of pristine HFP and functionalized HFP-18 membrane showing

their relative ductility and mechanical strength; and **(d)** I-V characteristics of HFP and HFP-18 membrane.....64

Figure 3.4: (a) Proton conductivity of HFP-12 and HFP-18 membranes as a function of temperature; (b) water uptake of sulphonated membrane (HFP-18) comparing the value of pristine HFP; (c) stacking pattern of fuel cell assembly; and (d) direct methanol fuel cell performance of HFP-18 and HFP-12 showing potential and power density as a function of current density.....67

Figure 4.1: (a) AFM images of both PVDF and nanohybrid (NH) before and after radiation. The arrows indicate the location of channels. Histogram shows the distribution of channel dimension; (b) SEM images of pristine PVDF and NH, before and after irradiation and bottom histogram indicate distribution of channel dimension.....78

Figure 4.2: **(a)** ¹H-spectra of pristine PVDF, PVDF-g-s and NH-g-s measured using 500 MHz magnetic field NMR. Respective proton positions are indicated in the chemical structure (inset) and spectrum; **(b)** FTIR spectra of the pristine PVDF, PVDF-g-s, NH and NH-g-s indicating various peak assigned peak positions; **(c)** FTIR -spectra of PVDF, NH , PVDF-g-s, and NH-g-s functionalize membrane and indicate the stretching vibration frequency of hydrophilic group (-OH) through the vertical line. **(d)** UV-vis absorption spectra of PVDF, NH, PVDF-g-s and NH-g-s showing the peak position by vertical lines; and **(e)** SEM images of PVDF-g-s and NH-g-s showing filling up of channels after grafting; and **(f)** AFM image after grafting of indicate specimens showing filling up after grafting and functionalization.....81

Figure 4.3 :(a) XRD patterns of indicate samples PVDF, PVDF-g, PVDF-g-s (lower column) and upper column show layered silicate dispersed specimen NH, NH-g, NH-g-s showing various crystalline planes; **(b)** Deconvoluted XRD patterns of PVDF-g-s and NH-g-s showing different phases; **and (c)** Polarizing optical microscope image of PVDF, NH, PVDF-g-s and NH-g-s showing spherulite in PVDF and mesh-like morphology in NH while needle like morphology after grafting and functionalization.....**84**

Figure 4.4: Thermal and electrical behavior of membranes **(a)** Thermograms of neat PVDF, NH and its grafted and sulphonated species (PVDF-g-s and NH-g-s); **(b)** DSC thermograms of PVDF/NH and their fictionalization membrane indicating the melting peak positions; **(c)** I-V measurement under DC electrical conductivity measurement; and **(d)** Water uptake values in percentage of the indicated membranes with error bars.....**85**

Figure 4.5:(a) Arrhenius plot (proton conductivity) k_m vs. $1/T$ for PVDF-g-s and NH-g-s; and **(b)** methanol permeability of indicated membranes comparing the standard Nafion117 values measured in similar condition.....**91**

Figure 4.6: (a) A schematic illustration of the setup employed for the fuel cell efficiency test (complete cell stack with MEA); **(b)** comparison of polarization curves of indicated membranes; and **(c)** power density as a function of current density of indicated membranes comparing the values of standard Nafion measured in similar condition.....**93**

Figure 5.1: (a) Details schematic presentation of ion bombardment followed by their functionalization (physical representations); and **(b)** reaction scheme of the PVDF and

nanohybrid grafting followed by the sulphonation (chemical representation).....100

Figure 5.2: (a) SEM micrographs of PVDF, PVDF-e, NH and NH-e, showing tiny nanochannels after etching; (b) the distribution of nanochannel diameter of the etched membrane as observed in SEM images; (c) AFM micrographs of PVDF, PVDF-e, NH and NH-e, indicating nanochannels after etching; and (d) the distribution of nanochannel diameter of the etched membrane as observed in AFM images.....101

Figure 5.3: (a) Proton NMR spectra of PVDF, PVDF-g-s and NH-g-s with magnified spectra in the inset in the similar chemical shift; (b) FTIR spectra of PVDF, PVDF-g-s, NH and NH-g-s in ATR mode indicating the absorption peak and crystalline structural peak position; (c) UV –visible spectra of PVDF, NH, PVDF-g-s and NH-g-s indicating the peak position; (d) SEM images of PVDF- g-s, NH-g-s after the grafting followed by the sulphonation showing the cover up of the nanochannel due to grafting; (e) AFM images of the PVDF-g-s, NH-g-s after the grafting followed by the Functionalization indicating filling of the nanochannels after grafting, and (f) Energy-dispersive X-ray spectroscopy (EDS) and elemental mapping of PVDF; and PVDF-g-s (functionalize membrane) indicating the presence of sulphur after functionalization.....105

Figure 5.4: (a) XRD patterns of PVDF, PVDF-g-s, NH and NH-g-s membranes showing crystalline planes; (b) deconvolution of the functionalized nanohybrid membrane indicating various phases; (c) Bar diagram of piezoelectric β -phase content of PVDF, PVDF-g-s, NH and NH-g-s membranes; (d) DSC thermograms of the indicated specimens mentioning the melting temperature through vertical lines; (e) Polarizing optical microscopic images of PVDF, PVDF-g-s, NH and NH-g-s

membranes showing spherulitic pattern in pure PVDF and mesh-like morphology in others; and **(f)** TGA thermograms of pure indicated specimens showing thermal stability of the membranes.....**107**

Figure 5.5: Electrochemical and potentiodynamic polarization studies of the membranes. **(a)** Nyquist plot of the indicated functionalized membranes (PVDF-g-s and NH-g-s); **(b)** Bar diagram showing the proton conductivity of the functionalized membrane (PVDF-g-s ,NH-g-s) at room temperature; **(c)** Proton conductivity of the functionalized membranes as a function of temperature; **(d)** Bode phase and modulus of PVDF-g-s ,NH-g-s membranes comparing Nafion117 as a function of frequency; **(e)** Tafel plot of blank, PVDF-g-s and NH-g-s at a concentration of 300 ppm; **(f)** Tafel plot of PVDF-g-s with concentration variation; **(g)** Tafel plot of NH-g-s with concentration variation.....**112**

Figure 5.6: Radionuclide sorption experiments and radiation emission studies using functionalized nanochannel membrane. **(a)** kinetics of Am⁺³ sorption studies using indicated functionalized membranes (PVDF-g-s and NH-g-s); **(b)** Bar diagram showing maximum uptake efficiency of different functionalized membranes; **(c)** Radiographic images of the radioactive loaded different membranes on C-39 detector (right side images are higher magnification of the corresponding left side images); **(d)** Deloading of adsorbed Am⁺³ ion in different complexing agents; **(e)** Schematic of the desorption of functionalized PVDF-g-s comparing with the NH-g-s membrane.....**115**

Figure 5.7: Complete fuel cell experiment using the developed membranes. **(a)** Proton conductivity of the indicated membranes as function of temperature; **(b)** water uptake of the functionalized membranes (PVDF, PVDF-g-s, NH, and NH-g-s); **(c)** Schematic presentation of membrane electrode assembly using developed membranes; **(d)**

Photograph of representative functionalized membrane showing its mechanical stability along with flexibility; **(e)** Polarization curves of PVDF-g-s and NH-g-s membranes comparing standard Nafion and open circuit voltage; and **(f)** Fuel cell performance in terms of power density as a function of current density using the functionalized membranes and comparison with standard Nafion.....119

Figure 6.1:Through nanochannel dimension are measured using SEM and AFM morphological investigations, **(a)** AFM images of pristine PVDF, NH, PVDF-e and NH-e showing the nanochannels by arrows under indicated fluence of Li⁺ ions bombardment; **(b)** the distribution of the nanochannel dimension as measured from the respective AFM images; **(c)** SEM images of pristine PVDF, NH, PVDF-e, and NH-e after the bombardment of Li⁺ ions at indicated fluence and the arrows show the location of the nanochannels; and **(d)** the distribution of nanochannel diameter after the irradiation followed by the chemical etching obtained from SEM images.....130

Figure 6.2: Represent the 3-D figure of the etched membrane with fluence variation, the PVDF-e (1×10⁶), PVDF-e (1×10⁷), NH-e (1×10⁶) and PVDF-e (1×10⁷) ions /cm² are shown in **(a)**, **(b)**, **(c)** and **(d)**, respectively. We are notifying that the channel dimension and no. of nanochannel is higher in case of the PVDF-7 and NH- 7 etched membrane.....131

Figure 6.3: Cross-sectional SEM of nanohybrid membrane before and after the styrene grafting followed by the sulphonation. **(a)** Low mag. SEM of NH-e **(b)** low Mag.SEM of NH-7 **(c)** High mag. SEM of NH **(d)** High Mag. SEM of NH-7.....132

Figure 6.4: The evidence of the grafting (using styrene monomer) followed by their sulphonation confirmed through different NMR nuclei studies, **(a)** the NMR spectra of

the PVDF-7, and NH-7 indicating the assignment of possible proton. **(b)** PDVF NMR spectra are given in the 6.4 **(b)** and PVDF-6 and NH-6; **(c)** ¹³C-NMR of the functionalized and un-functionalized membrane. In ¹³C-NMR the three new peaks at chemical shift 118.7, 121.9 and 127.6 ppm indicate the grafting of the styrene monomer on the back bone of the PVDF chain.**(d)** F-19 NMR of the pristine PVDF and its Functionalized (NH-7) membrane.....**134**

Figure 6.5: **(a)** FTIR spectra of PVDF, NH, PVDF-7, and NH-7 indicating the possible bands for different functionalities and crystalline structure; **(b)** UV spectra of indicated samples, before and after functionalization; and **(c)** Surface morphology through AFM after graft and functionalization showing the coverage of the nanochannels.....**136**

Figure 6.6: Characterization of membrane materials and to provide evidence of the formation of the electro active (piezoelectric) β-phase and thermal stability. **(a)** XRD patterns of PVDF, NH, PVDF-6, NH-6, PVDF-7 and NH-7; **(b)** Deconvolution of a representative XRD spectra of NH-7 showing different phase fraction; **(c)** Piezoelectric β-content of the different membranes, calculated from the respective deconvulated patterns; **(d)** DSC thermograms of PVDF, NH, PVDF-6, NH-6, PVDF-7 and NH-7 showing the respective melting temperatures; **(e)** Polarizing optical microscopic images of PVDF, NH, PVDF-7 and NH-7; and **(f)** TGA thermograms of PVDF, NH, PVDF-6, NH-6, PVDF-7 and NH-7, indicate their respective degradation temperatures.....**139**

Figure 6.7: Characteristic parameters of the hydrophilic membranes as developed **(a)** Water uptake of the indicated membranes; **(b)** Ion exchange capacity, mmoles/g of the functionalized membranes estimate using the radioactive nuclide CsCl; **(c)** Nyquist Plot

of indicated membranes; **(d)** Bode phase and Bode modulus as a function of frequency of indicated functionalized membranes; **(e)** Proton conductivity variation with temperature of the different membranes as indicated; and **(f)** Arrhenius plot of different membranes for the estimation of activation energy.....142

Figure 6.8: Fundamentals of radioactive waste management and the morphology of the functionalized membranes **(a)** Kinetics of sorption of the radioactive Am^{+3} ions using the indicated membranes; **(b)** Uptake of the radioactive Am^{+3} ions comparing with pristine PVDF/NH; **(c)** Radiography of the indicated membranes on the C-39 detector after the uptake measurements; **(d)** Schematic of the alpha spectrometry measurement and energy loss from the different regions; **(e)** the depth profiles of ion exchangeable groups present in the nanochannels for Li^+ membranes showing fluence dependency in PVDF and its nanohybrid; and **(f)** Comparison of Ag^+ and Li^+ ion induced membranes showing the relative depth profile of PVDF and NH irradiated with 1×10^6 fluence.....144

Figure 6.9: Alpha spectrum of the $^{241}Am^{3+}$ Loaded Functionalized membranes **(a)** spectrum recorded side one of membrane; **(b)** spectrum recorded second side of membrane; **(c)** overlap alpha spectrum of the PVDF-6 membrane: the alpha spectrum both side of the Li-ions bombardment, selective chemical etching subsequent grafting of the styrene conducting monomer followed by the sulphonation were recorded and found almost similar pattern of the alpha spectrum, which is conclude that through nanochannel formed. The details of fluence, ions and nanoclay variation explanation in manuscripts. In figure **(c)** exact overlap indicate the formation of the through nanochannels.....148

Figure 6.10: (a) The schematic arrangement for the measurement of pulse height spectrum; (b) a comparison of pulse height spectrum along with the background spectrum; and (c) comparative study of the Ag^+ and Li^+ irradiated pulse height spectra of functionalized PVDF-6 PVDF-7 membranes at two different fluence.....150

LIST OF TABLE

Table 1.1: Classification of the fuel cell devices based on fuel, electrolytes and operating temperature.....	23
Table 1.2: Channel diameter after etching process of Sn exposed on the piezoelectric β -phase PVDF thin foils at oxidizing agent 0.25 mol L ⁻¹ aqueous KMnO ₄ solutions with various alkaline conc.....	33
Table 1.3: Results of the etching of the PVDF films which were irradiated with various ions and fluence.....	33
Table 1.4: Ionic membrane characteristics of the various functionalized membrane materials.....	34
Table 1.5: Comparative Fuel cell efficiency of the various membrane electrodes stack.....	35
Table 3.1: Comparison of proton conductivity (K^m), methanol permeability (P), Activation Energy (E_a) and selectivity parameter (SP) of HFP-12 and HFP-18 with the standard Nafion117 membrane at 25°C and 50% water-methanol mixture.....	66
Table 4.1: Conductivities ($k^m \times 10^{-2}$ S cm ⁻¹) of indicated membranes (functionalized PVDF and nanohybrid) at different temperatures.....	88
Table 4.2: Membrane conductivity (k^m), methanol permeability (P) at 30 °C, energy of activation (E_a) and power density values for different membranes measured at 30 °C using 30% methanol water mixture.....	89

Table 6.1: The membrane characteristics such as, ion exchange capacity (IEC), water uptake (WU), and activation energy (Ea) and proton conductivity (km) of the functionalized membranes.....142

LIST OF SCHEMES

- Scheme 1.1:** Chemical representation synthesis of functionalized membrane (PVDF) through direct and pre-irradiation tagging of styrene monomer followed by sulfonation.....12
- Scheme 4.1:** Schematic representation of the swift heavy ions irradiation on polymer membrane, followed by selective chemical etching on irradiated membrane subsequent grafting within the nanochannels followed by sulphonation. Bottom column indicate the grafting reaction within the nanochannel followed by its sulphonation to make the nanochannel conducting.76
- Scheme 6.1:** Schematic presentation of the irradiation, nanochannel formation, grafting followed by the sulphonation to generate a functionalized membrane.....128
- Scheme 6.2:** Schematic representation chemical reactions of the ion beam bombardment (Li^+ beam) which generate reactive sites (free radicals) followed by grafting using styrene monomer and subsequently the sulphonation using chlorosulphonic acid. This functionalization converts the nano-dimensional channels into conducting for the ions transport and radionuclide capturing experiments.128

LIST OF ABBREVIATIONS

PEM	Proton electrolyte membrane
AEMs	Anion Exchange membranes
CEMs	Cation exchange membranes
BPMs	Bipolar membranes
PFSA	Perfluorosulfonic acid
DMFCs	Direct methanol fuel cells
MEA	Membrane electrode assembly
PEMFCs	Polymer electrolytes Fuel cell membrane.
PVDF	Poly (vinylidene fluoride)
OCV	Open circuit voltage
PTFE	poly(tetrafluoro ethylene)
PVDF-HFP	poly(vinylidene fluoride-co- hexafluoro propylene)
PVDF-CTFE	poly(vinylidene fluoride-co- tetrafluoro ethylene)
SHI	Swift heavy ions
LET	Linear energy transfer
NH	Nanohybrid
PSSA	Polystyrene sulfonic acid
MeV	Mega electron volts
PS	Polystyrene
DS	Degree of sulfonation
IEC	Ion exchange capacity
WU	Water uptake
3-HT	3 -hexyl-thiophene

P3HT	poly(3 hexylthiophene)
DCM	Dichloromethane
GPSC	General Purpose scattering chamber
SRIM	Stopping range of ions in materials
DMF	Dimethyl formamide
PVDF-s	Direct sulphonation poly(vinylidene difluoride),
PVDF-NH-s	Direct sulphonation of the PVDF nanohybrid membrane
QAPPESK	Quaternizedpoly(phthalazinon ether sulfone ketone
QAPVA	Novel cross-linked quaternized poly (vinyl alcohol) (PVA)
FEP-g-PVBTMAOH	The radiation-grafting of vinyl benzyl chloride onto poly (hexafluoropropylene-co-tetrafluoroethylene)
QPPESEN	Quaternized phenolphthalein based poly(arylene ether sulfone nitrile)
FPAES-Im-52	Fluorene-containing poly(arylene ether sulfone)s with imidazolium groups
SP	Selectivity parameter

Symbols	Description
α	Alpha
β	Beta
γ	Gamma
δ	Delta
T	Trans
G	Gauche
Å	Angstrom
μm	Micro meter
nm	Nano meter

θ	Angle
ρ	Resistivity
σ	Conductivity
d	Interplanar spacing
V	Volt
A	Ampere
Mm	Mili meter
cm	Centi meter
g	Gram
$^{\circ}\text{C}$	Temperature
I_{max}	Current Density
P_{max}	Power Density
mW	Mili watt
mA	Mili ampere
Ea	Activation energy
P	Methanol permeability
S	Siemens

PREFACE

Membrane technologies have been the key component of research in the last few decades, with the latest improvement in both fabrication and design aspects. Porous / nanochannel polymeric membranes have gained much attention in this perspective for their utilization in a variety of fields such as adhesive, sensor, biotechnology, waste water treatment including separation techniques and ion exchange membranes for polymer electrolytes membrane fuel cell (PEMFCs), because of their excellent thermal, outstanding mechanical properties along with electrical properties when suitably functionalized with some functional group.

This thesis mainly focuses the research work being conducted on fabricating porous polymer membranes followed by the functionalization and subsequently their applications in fuel cell technology as electrolytes membrane and Functionalized membrane used for the waste water treatment mainly in the radionuclide tracing. In this context, swift heavy ions (SHI) bombardment on the polymeric membrane design the porous membranes having controlled channels dimension using ions of different size, nanoparticles and fluence variation. The effect of SHI on the polymeric membrane creates the reactive sites (free radicals), which are utilized to functionalize for relevant applications. However, this thesis aims to discuss the fabrication of latent track/nanochannels in polymer membrane and subsequent functionalization for energy applications, especially in fuel cell technology.

The thesis consists of seven chapters; in the first chapter, we will discuss a brief introduction of the polymeric membrane, materials like PVDF and its copolymer and their conformations, Radiation-induced grafting (Swift heavy ions). A detailed literature survey

has been carried on fuel cell technology and the effect of the SHI on the polymer. In the second chapter, detail of materials, experiments, characterizations technique and measurements are discussed. In third chapter functionalized (sulphonates) the PVDF-HFP polymer membrane using chlorosulphonic acids and measures the DMFCs efficiency. In the fourth chapter of the thesis, swift heavy ions, Silver ions 120 MeV energy and 5×10^7 ions /cm² fluence irradiated PVDF and its nanohybrid film followed by the chemical etching subsequent grafting with the help of the conducting monomer 3-Hexyl thiophene and sulphonation carried out grafted species make the nanochannel / latent track into conducting nanochannel for the ions transport. Furthermore, the functionalized membrane assembled Fuel cell stack and measure cell efficiency. In the fifth chapter, Silver ions with fluence 1×10^7 ions/cm² irradiated on the polymer film followed by the styrene monomer grafting sulphonation subsequently for the purpose of the fuel cell membrane and radionuclide tracing and in the sixth chapter, lithium ions irradiation with two fluences 1×10^7 and 1×10^6 ions/cm² and grafting of the styrene monomer followed by ionic group tagging for low waste radionuclide sensing and finally in the last chapter (seventh) gives significant observations, conclusions and suggestions of the future work.